A study of the Fermi surfaces of lithium and disordered lithium-magnesium alloys: theory and experiment

1993 J. Phys.: Condens. Matter 5 6419

(http://iopscience.iop.org/0953-8984/5/35/007)

J. Phys.: Condens. Matter 5 (1993) 6419–6432. Printed in the UK

A study of the Fermi surfaces of lithium and disordered lithium–magnesium alloys: theory and experiment

S S Rajput†, R Prasad†, R M Singru†, W Triftshäuser‡, A Eckert‡, G Kögel‡, S Kaprzyk§‖ and A Bansil§

† Department of Physics, Indian Institute of Technology, Kanpur 208016, India
‡ Institut für Nukleare Festkörperphysik, Universität der Bundeswehr München, 8014 Neubiberg, Federal Republic of Germany
§ Department of Physics, Northeastern University, Boston, MA 02115, USA

Received 10 February 1993

Abstract. We present a theoretical and experimental study of the Fermi surfaces (FSs) of Li and the disordered alloys $Li_{1-x}Mg_x$ ($0.6 \geqslant x > 0.0$) in the BCC phase. Theoretical calculations employ the first-principles fully charge-self-consistent Korringa–Kohn–Rostoker coherent-potential-approximation scheme within the local-density approximation. The experiments involve the two-dimensional angular correlation of positron annihilation radiation measurements on four $Li_{1-x}Mg_x$ single-crystal specimens with $x = 0.0$, 0.28, 0.40 and 0.60. Good overall agreement is found between experiment and theory with regard to the size and shape of the FS as x is increased from 0.0 to 0.6, although some discrepancies are noted. The question of the critical Mg concentration $x = x_c$ at which the FS first makes contact with the Brillouin zone boundary in $Li_{1-x}Mg_x$ alloys is considered in some detail.

1. Introduction

The electronic structures and Fermi surfaces (FSs) of Li and Li–Mg alloys have invoked considerable interest in recent years. The FS of pure Li metal shows a small but definite departure from a free-electron sphere, and a study of its asphericity thus provides a delicate test of band theory predictions. However, because of the presence of a martensitic phase transformation, Li goes into a mixed BCC–HCP phase for $T < 80$ K (Young and Ross 1984). Therefore, a measurement of the FS of Li in the BCC phase using the conventional methods such as the de Haas–van Alphen (DHVA) effect which require the specimen to be cooled to very low temperatures is not possible. A partial solution to this problem was offered by Randles and Springford (1976) who measured the DHVA effect in samples containing a polycrystalline dispersion of randomly oriented Li spheres of small size. Although these studies provide an estimate of the radial distortion of the FS in BCC Li, they do not determine the FS dimensions directly.

Several other experimental studies of BCC Li have been performed using Compton scattering (Cooper *et al* 1965, 1970, Phillips and Weiss 1968, 1972, Eisenberger *et al* 1972, Wachtel *et al* 1975, Berndt and Brümmer 1976, Schülke *et al* 1984, Sakurai *et al* 1992) and positron annihilation techniques (Stewart 1964, Donaghy and Stewart 1967, Paciga and Llewelyn Williams 1971, Basinski *et al* 1979, Manuel *et al* 1982, Oberli *et al* 1985a, b)

‖ Present address: Academy of Mining and Metallurgy, Institute of Physics and Nuclear Techniques, Krakow, Poland.

0953-8984/93/356419+14$07.50

because these measurements can be carried out above 80 K, and these spectroscopies can provide valuable information about the FS. Theoretical calculations of the band structure and FS of Li have been reported by several workers using a variety of established band-structure methods (see, for example, the references compiled in table 1, reported by Randles and Springford (1976)).

Table 1. Characteristic features of the band structure of Li.

	Theory		
Physical quantity	Present work	Other work	Experiment
$E_P - E(\Gamma_1)$ (eV)	3.41	(1) 3.54–3.55[a] (2) 3.45[b] (3) 3.85[c]	Not available
$N(E_F)$ (states eV^{-1}/atom)	0.488	(1) 0.516[a] (2) 0.481[b] (3) 0.477[c] (4) 0.480[d]	Not available
'Band gap' $E(N_1') - E(N_1)$ (eV)	2.81	(1) 2.84–2.90[a] (2) 2.78[b] (3) 2.88[c]	2.0 ± 0.1[e]

[a] APW method by Dagens and Perrot (1973).
[b] LCAO method by Ching and Callaway (1974).
[c] APW method by Bross and Bohn (1975), with the screening parameter $\kappa = 0.9\kappa_0$.
[d] KKR method by Moruzzi *et al* (1978).
[e] Mathewson and Myers (1973); see discussion in the text, in section 3.

The $Li_{1-x}Mg_x$ alloys form solid solutions of Mg in the BCC Li lattice over a wide Mg concentration range ($x = 0.0$–0.7) and above $x = 0.85$ they form a solid solution of Li in the HCP Mg lattice (Roberts 1960). In the BCC structure the average number of valence electrons in $Li_{1-x}Mg_x$ can be continuously varied in the range $x = 1.0$–1.7 by substituting Mg for Li atoms; the lattice constant varies slowly in the range $a = 6.610$–6.648 au with a slight minimum at around $x \simeq 0.4$ (Herbstein and Averbach 1956). The $Li_{1-x}Mg_x$ alloys are, therefore, a unique system in nature to verify theoretical electronic structure models experimentally. Notably, the interest in the Li–Mg system is also driven by the fact that these alloys are among the lightest commercially available structural materials, with technological applications in the transportation and aerospace industries because of their high strength-to-weight ratios (Raynor 1959, Polmear 1981).

Turning to the FS of Li–Mg alloys, note that, according to the nearly free electron model, we expect the almost spherical FS of Li to expand with increasing Mg concentration x and to make contact with the Brillouin zone (BZ) boundary at some critical concentration $x = x_c$. This behaviour has not been confirmed via direct measurement so far because the conventional methods of fermiology, such as the DHVA effect, cannot generally be used in concentrated alloys where electrons develop finite lifetimes owing to disorder scattering of states. Additionally, as in the case of Li, the presence of phase transformations in $Li_{1-x}Mg_x$ at low temperatures rules out FS measurements for the BCC phase below $T = 100$–160 K (depending on x (Oomi and Woods 1985)). The experimental techniques such as Compton scattering (Cooper 1985) or the angular correlation of positron annihilation radiation (ACAR) (Berko 1983), which involve the determination of the momentum distribution, are not sensitive to electron lifetimes and thus are best suited to investigating the disordered phases.

Berndt and Brümmer (1976) have measured the Compton profiles of $Li_{1-x}Mg_x$ ($x = 0.0$–0.7) but their measurements did not provide any useful information about the FS dimensions because they used polycrystalline samples and moderate momentum resolution. In contrast, the two-dimensional (2D) ACAR measurements using single crystals appear more promising owing to the higher available angular resolution, and the 2D nature of the data (Berko 1983).

The electronic structure of $Li_{1-x}Mg_x$ alloys has been investigated theoretically by Callcot *et al* (1980) and Bruno *et al* (1987) using the Korringa–Kohn–Rostoker (KKR) coherent-potential approximation (CPA). However, neither of these calculations appears to have employed a charge self-consistent scheme. Callcot *et al* (1980) have compared their KKR CPA results for the soft-x-ray emission spectra from $Li_{0.8}Mg_{0.2}$ with experiment but have not presented any results for the FSs of $Li_{1-x}Mg_x$ alloys. Bruno *et al* (1987) computed the FSs of the $Li_{1-x}Mg_x$ alloys using the KKR CPA and compared the computed FS neck radii for $x = 0.44$, 0.51 and 0.58 with the results of optical experiments. Observing systematic differences, Bruno *et al* (1987) suggested that a more realistic comparison between theory and experiment could be made via ACAR data; however, no ACAR measurements on $Li_{1-x}Mg_x$ were available in 1987 for such a comparison.

Bearing these considerations in mind, we were motivated to undertake the present theory–experiment study of the FS of $Li_{1-x}Mg_x$ alloys. The KKR CPA methodology is used on the theoretical side, while the experiments involved 2D ACAR spectroscopy. The FSs of $Li_{1-x}Mg_x$ have been calculated for $x = 0.0$, 0.14, 0.22, 0.28, 0.40 and 0.60 using the all-electron fully charge self-consistent KKR CPA method which has already provided a satisfactory theoretical description of the FSs of several disordered alloys. The theoretical results are compared with the dimensions of FSs determined via high-resolution 2D ACAR measurements made on single crystals of $Li_{1-x}Mg_x$ for $x = 0.0$, 0.28, 0.40 and 0.60. The plan of the present paper is as follows. In section 2 we give an overview of the relevant calculational procedures used and the details of the present 2D ACAR experiments. The theoretical and experimental results are presented and discussed in section 3. Conclusions are summarized in section 4.

2. Methods

2.1. Calculational procedure

The electronic structure of Li and the disordered $Li_{1-x}Mg_x$ ($x = 0.14$, 0.22, 0.28, 0.40 and 0.60) alloys were calculated using the all-electron fully charge self-consistent KKR CPA method described in detail elsewhere (see, e.g., Bansil (1982, 1987, 1993), Stocks and Winter (1984), Mijnarends (1987), Prasad (1991) and Bansil *et al* (1992)). In the limit $x = 0.0$ of pure Li, this method reduces to the KKR method of band theory. Briefly, in the KKR CPA method, the disordered alloy is replaced by an ordered array of effective atoms whose scattering properties are determined by a self-consistency condition. Within the density functional theory, the KKR CPA method provides a first-principles parameter-free theory of the electronic structure of disordered alloys. In the present work we have used the local-density approximation and the exchange–correlation potential of von Barth and Hedin (1972). The only inputs for the calculation were the atomic numbers of Li ($Z = 3$) and Mg ($Z = 12$) and the lattice constants taken from Levinson (1958). To begin with, the muffin-tin potentials for each constituent in each alloy were generated on the given lattice using overlapping charge densities. The self-consistency equation, in the framework of KKR CPA formalism, was solved by an iterative method. The resulting charge densities were used to generate the new muffin-tin potentials. The whole procedure was iterated until

charge self-consistency was achieved. The level of self-consistency Δ (i.e. the integrated difference between input and output charge densities) was less than 10^{-4} electrons; the Fermi energy E_F converged to about 10^{-4} Ryd (see Kaprzyk and Bansil (1990) and Bansil and Kaprzyk (1991) for specific working details of our KKR CPA methodology).

It is well known that unlike that of a pure metal the FS of an alloy is not sharp (see, e.g., Prasad *et al* (1981)), but that the FS acquires a width arising from the disorder-induced scattering of electrons. The spectral density function $A(\boldsymbol{k}, E_F)$, where E_F denotes the Fermi energy, is a sharp delta function for pure metals but generally becomes broadened for alloys. The half-width at half-maximum of the function $A(\boldsymbol{k}, E_F)$ is a measure of the broadening of the FS. In the present work the FS of disordered $Li_{1-x}Mg_x$ alloy was calculated by locating the position of the peak in the spectral density function $A(\boldsymbol{k}, E_F)$.

2.2. *Experimental details*

The present 2D ACAR measurements were carried out with a system consisting of two high-density avalanche chambers with a geometrical resolution (FWHM) of 1.5 mm × 1.5 mm for each detector element. Each chamber contained an active area of 30 cm × 30 cm and was placed 10 m away from the single-crystal specimen under study. The detectors, manufactured by Oxford Positron Systems, possessed a detection efficiency of 3% for 511 keV annihilation photons. The coincidence time resolution (FWHM) of the detectors was 44 ns, thus resulting in a low accidental coincidence rate. The dead time was less than 4 μs with the fast data acquisition system employed. Positrons emitted by a 15 mCi ^{22}Na line source were focused onto the specimen by a superconducting magnet (strength, 5.2 T). The total angular resolution (FWHM) of the system, without the contribution due to the thermal motion of the positron, was 0.5 mrad × 0.23 mrad as determined from the observed width of the positronium peak for a quartz single crystal (Berko *et al* 1977).

Single crystals of $Li_{1-x}Mg_x$ were drawn using a modified Bridgman method; the purities of the starting materials (Li and Mg) were 99.99%. The specimens were cut by spark erosion into cubes of 10 mm length and kept in silicone oil. A clean surface of the crystals was obtained by etching and polishing in a mixture of ethanol, methanol and 1–3% of concentrated nitric acid. The handling and mounting of the crystals into the sample holder were performed in a high-purity argon atmosphere; the crystals were kept in a high vacuum during the measurements. Other working details of our 2D ACAR set-up have been described elsewhere (Eckert 1989).

The 2D ACAR distributions $N(p_x, p_y)$ were measured for four $Li_{1-x}Mg_x$ samples with $x = 0.0, 0.28, 0.40$ and 0.60. The samples were oriented such that the integration direction p_z lies along the [110] direction; the typical total number of counts taken for each specimen was 1.5×10^7 for each sample. It was established that cooling the sample to 160 K resulted in only a slight improvement in the momentum resolution compared with the room-temperature data. All the measurements were, therefore, carried out at room temperature. The data were corrected for the finite detector size via an experimentally determined correction matrix. By applying a 'reconstruction' method to the measured data $N(p_x, p_y)$, the three-dimensional two-photon momentum distribution $\rho^{2(\gamma)}(\boldsymbol{p})$ was obtained. A preliminary report of the present measurements has been given elsewhere (Triftshäuser *et al* 1992).

3. Results and discussion

Table 1 considers characteristic features of the band structure of Li. Our computed values of the band width $E_F - E(\Gamma_1)$ as well as the density $N(E_F)$ of states at the Fermi energy

compare well with other calculations. Our theoretical value of the band gap $E(N_1')-E(N_1)$ compares reasonably with the results of other calculations, but these theoretical values are all larger than the value of 2.0 eV deduced from optical measurements; a similar observation concerning this band gap has also been made by Bruno *et al* (1987) in connection with their calculations on $Li_{1-x}Mg_x$ alloys.

Figure 1 shows the FSs calculated by us for pure Li and $Li_{1-x}Mg_x$ alloys and it is seen that the FS of Li is a slightly distorted sphere, with the largest deviation from the free-electron sphere being observed as a bulge along the [110] axis (figure 1(*a*)). The distortion in the FS can be described through the parameter (Ching and Callaway 1974)

$$\eta(\hat{k}) = 10^4[k_F(\hat{k}) - k_F^0]/k_F^0 \tag{1}$$

where $\hat{k}$ denotes a particular direction in the momentum (k) space, $k_F(\hat{k})$ the FS dimension along the $\hat{k}$ direction, and k_F^0 the radius of the free-electron Fermi sphere. Our calculations give $\eta[100] = -227$, $\eta[110] = 338$ and $\eta[111] = -97$. These values agree closely with the results of Ching and Callaway (1974) who used the method of the linear combination of atomic orbitals (within the local-density approximation) and obtained $\eta[100] = -220$, $\eta[110] = 380$ and $\eta[111] = -110$.

We see from figure 1(*a*) that the FS of Li does not touch the BZ boundary. In $Li_{1-x}Mg_x$ alloys, the e/a ratio increases with increasing Mg concentration, and we expect the FS to expand and touch the BZ boundary first along the [110] direction. An interesting question which has been the subject of numerous studies is what the critical Mg concentration $x = x_c$ is at which the FS first makes contact with the BZ boundary. Early 1D ACAR work of Stewart (1964) suggested $x_c = 0.19$. A value of $x_c = 0.19$ was also proposed from the analysis of magnetic susceptibility data (Svechkarev *et al* 1977). On the other hand, measurements of physical quantities such as the Hall voltage (Ide 1971), optical properties (Mathewson and Myers 1973) and Knight shifts (Lynch *et al* 1973) indicated that $x_c \geqslant 0.30$. Using their Compton profile data for the Li–Mg alloys, Berndt and Brümmer (1976) concluded that x_c lies in the range 0.3–0.4. Egorov and Fedorov (1983) measured the thermopower and resistivity of $Li_{1-x}Mg_x$ alloys for $0.4 \geqslant x \geqslant 0.0$ at various temperatures and concluded that their observed value of $x_c = 0.2$ agreed well with the value $x_c = 0.247$ calculated by Vaks *et al* (1981). Varlamov *et al* (1989) have made a detailed experimental study of the temperature dependence of the differential thermopower and specific conductivity in $Li_{1-x}Mg_x$ and concluded that their results are also in good agreement with the theoretical value (Vaks *et al* 1981) of $x_c = 0.247$.

It thus appears that different experimental and theoretical methods lead to a range of values of x_c. Part of this behaviour has been attributed by Varlamov *et al* (1989) to the presence of mixed phases below the martensitic phase transformation temperature T_M and to the fact that the value of T_M depends on x. The effect of smearing of the FS on alloying can further complicate the problem. As noted above, the FSs of alloys possess a finite width arising from the disorder scattering of electrons. This is indicated in figures 1(*b*)–1(*f*), where the shape of the theoretical FSs, obtained in the $(1\bar{1}0)$ plane passing through Γ, is drawn for different values of x. The central curves in these figures correspond to the peak positions of the spectral density function $A(k, E_F)$, while the inner and outer envelopes correspond to k-values where $A(k, E_F)$ is reduced to half its value at the peak. Obviously, as the FS swells upon adding Mg, the outer envelope first touches the BZ boundary; this is seen to occur from figure 1(*b*) at $x_1 = 0.14$, while the inner envelope touches the BZ boundary at $x_2 = 0.22$ (figure 1(*c*)). A well defined neck in the FS appears to be formed for $x > 0.22$ (figures 1(*d*)–1(*f*)). The present theoretical results, therefore, indicate that the

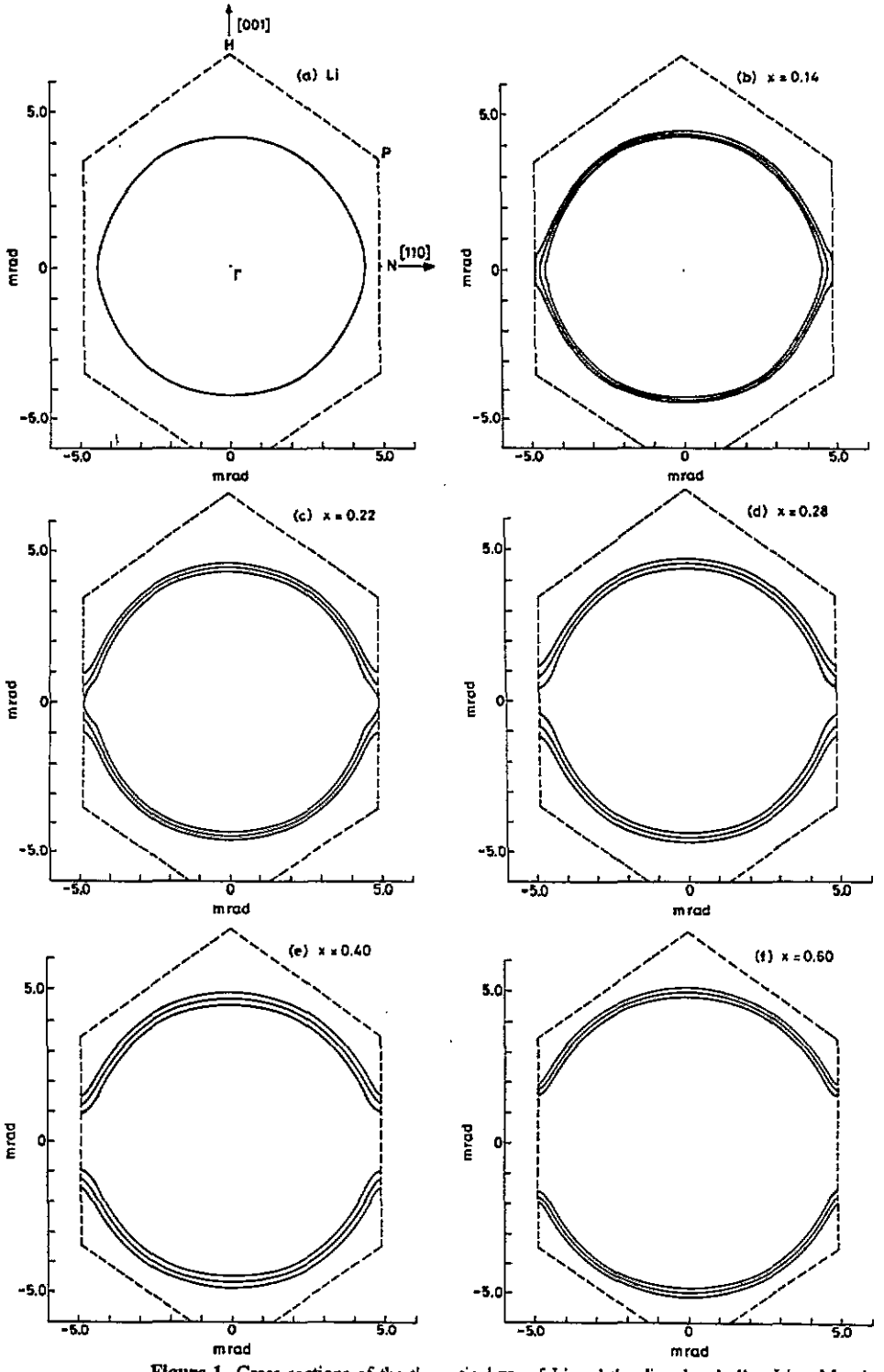

Figure 1. Cross sections of the theoretical FSs of Li and the disordered alloy $Li_{1-x}Mg_x$ in the $(1\bar{1}0)$ plane passing through Γ: (*a*) Li; (*b*) $x = 0.14$; (*c*) $x = 0.22$; (*d*) $x = 0.28$; (*e*) $x = 0.40$; (*f*) $x = 0.60$. The BZ boundaries are also shown. The momentum scale is in milliradians (1 mrad = 0.137 au).

FS of $Li_{1-x}Mg_x$ touches the BZ in the range $0.22 \geqslant x \geqslant 0.14$; this perhaps explains the wide range of x_c-values observed by various measurements, since different experimental techniques would generally sample the spectral density function differently.

Further insight into changes in the FS topology is provided by figure 2 which gives the cross sections of the FSs of $Li_{1-x}Mg_x$ in the HPHP face of the BZ centred at N for $x = 0.22$, 0.28, 0.40 and 0.60. These results emphasize the shape of FS neck on the HPHP face and indicate the growth of neck size with increasing Mg concentration.

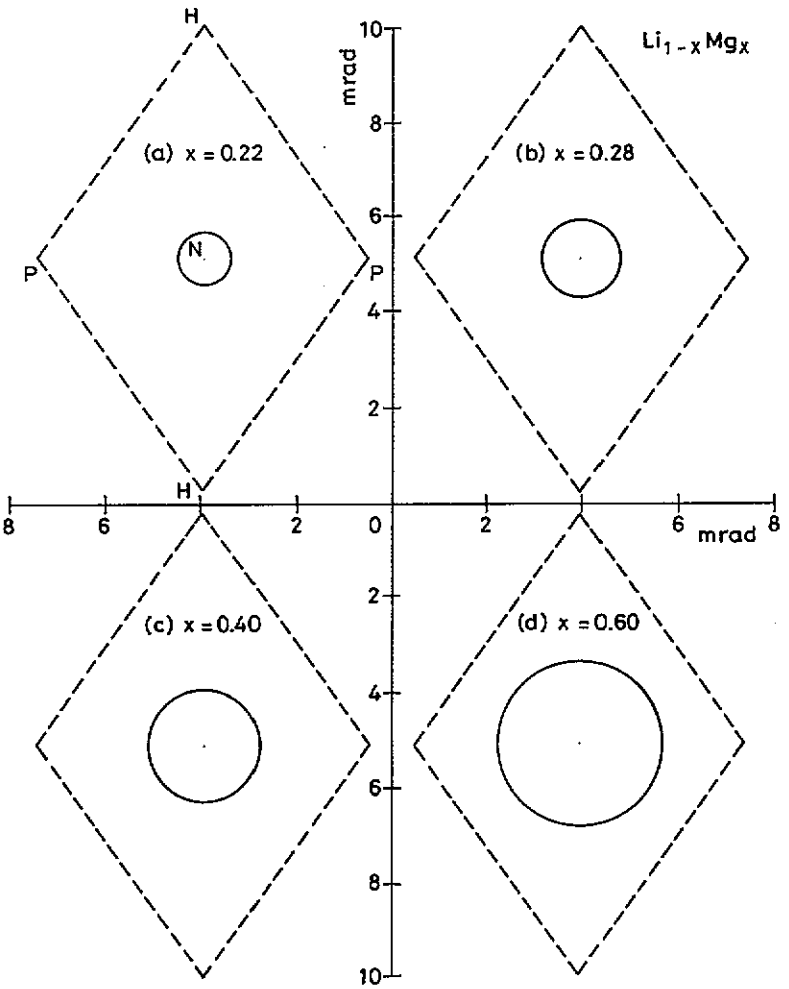

Figure 2. Cross section of the theoretical FS of the disordered alloy $Li_{1-x}Mg_x$ in the HPHP face centred at N of the BZ for (*a*) $x = 0.22$, (*b*) $x = 0.28$, (*c*) $x = 0.40$ and (*d*) $x = 0.60$.

We now compare our theoretical predictions with the 2D ACAR measurements. In this connection, we emphasize that we observe for $Li_{1-x}Mg_x$ a single positron lifetime τ for $0.0 \leqslant x \leqslant 0.6$ (figure 3). The fact that the τ-values in figure 3 possess bulk-like values in the range 230–275 ps indicates that in our samples the positron was not significantly trapped at intrinsic defects, and that the present 2D ACAR data are representative of the momentum

density of the Bloch-like delocalized states. The essentially linear dependence of τ on x shows that the positron does not possess a preferential affinity for either of the constituent atoms in the Li-rich alloys; interestingly, Kubica *et al* (1975) suggest that in the Mg-rich regime the positron annihilates preferentially from Li-clusters.

We emphasize that it was not our aim in this work to reconstruct the full three-dimensional two-photon momentum distribution $\rho^{2\gamma}(\boldsymbol{p})$ from experiment, nor to compare the results with band theory predictions, as has been done, for example, for V (Pecora *et al* 1988) and Mg (Kontrym-Sznajd 1992). Rather our main aim was to examine changes in the FS dimensions of $Li_{1-x}Mg_x$ alloys in the light of KKR CPA calculations and 2D ACAR experiments. Keeping this in mind, our procedure for determining the Fermi radii $k_F(\hat{\boldsymbol{k}})$ from the measured 2D ACAR curves was as follows. In the spirit of the analysis of Li by Donaghy and Stewart (1967), Oberli *et al* (1985a, b) and Stewart (1986), a phenomenological model containing three terms was chosen to represent $\rho^{2\gamma}(\boldsymbol{p})$. These three terms consisted of

(i) a centrally situated free-electron sphere of radius k_F^0 which describes the annihilation with conduction electrons,

(ii) an anisotropic contribution by high-momentum components described in terms of 12 three-dimensional Gaussian functions centred at $\boldsymbol{H} = (\pm\pi/a, \pm\pi/a, 0)$, $(\pm\pi/a, 0, \pm\pi/a)$ and $(0, \pm\pi/a, \pm\pi/a)$ where a denotes the lattice constant and

(iii) a centrally located Gaussian distribution which describes the annihilation with core electrons.

The next step involved a 'reconstruction' of $\rho^{2\gamma}(\boldsymbol{p})$ from the 2D ACAR data set $N(p_x, p_y)$ (Mijnarends 1977, Pecora 1989). The specific scheme consisted of expanding $\rho^{2\gamma}(\boldsymbol{p})$ into cubic harmonics $F_{ln}(\Omega)$ (Mijnarends 1969) and testing the fidelity of reconstruction with the help of the above model. Since, as noted, our main purpose was the determination of $k_F(\hat{\boldsymbol{k}})$, the reconstructed $\rho^{2\gamma}(\boldsymbol{p})$ was folded back into the $\boldsymbol{k}$-space by following the Lock–Crisp–West (1973) procedure:

$$\rho^{2\gamma}_{\mathrm{LCW}}(\boldsymbol{k}) = \sum_{\boldsymbol{H}} \rho^{2\gamma}(\boldsymbol{k} + \boldsymbol{H}) \tag{2}$$

where $\boldsymbol{H}$ denotes the reciprocal-lattice vectors. The sum over $\boldsymbol{H}$ was carried out up to $|\boldsymbol{p}| = 15$ mrad so that the contribution from the high-momentum components (i.e. the 12 nearest neighbours in the reciprocal lattice) was included; Oberli *et al* (1985b) have shown that the anisotropic contribution from the high-momentum components is negligible beyond $|\boldsymbol{p}| = 15$ mrad. Using an iterative method, a criterion for determining $k_F(\hat{\boldsymbol{k}})$ from the Lock–Crisp–West $\boldsymbol{k}$-space occupational density $\rho^{2\gamma}_{\mathrm{LCW}}(\boldsymbol{k})$ was developed so that k_F^0 could be recovered faithfully and self-consistently from the model $\rho^{2\gamma}(\boldsymbol{p})$.

The accuracy of our procedure for determining FS radii deserves some comment, especially since only one 2D ACAR projection (with integration along the [110] direction) was involved in the analysis. While a detailed study of this question, including a discussion of the effects of using more than one data projection, is taken up elsewhere (Eckert 1989), we summarize some of the salient results as follows. The average error in determining the FS radius $k_F(\hat{\boldsymbol{k}})$ with the present 2D ACAR data is estimated to be about 1% or ± 0.05 mrad. The statistical error Δk_F^0 is about 0.2%. We note that our three-term model for $\rho^{2\gamma}(\boldsymbol{p})$ does not include enhancement effects associated with e^+–e^- many-body correlations. We estimate, however, that the neglect of these effects probably introduces an uncertainty into the $k_F(\hat{\boldsymbol{k}})$-values of less than 0.2%. A similar conclusion was reached by Oberli *et al* (1985a). For these reasons, we did not attempt to modify our procedures for FS determination in order to incorporate enhancement effects.

The variation in anisotropy $\eta(\hat{k})$ in going from the [110] to the [001] direction (via the [111] direction) in Li is shown in figure 4. The experimental results of Oberli *et al* (1985a, b) and the calculations of MacDonald (1980) (using the non-local self-energy approximation) are also shown. In examining figure 4 we must remember that the FS distortions are quite small in absolute magnitude, and that we have used a large scaling factor of 10^4 in equation (1) defining $\eta(\hat{k})$. The maximum anisotropy from the present 2D ACAR data is $\delta = [k(110) - k(001)]/k_F^0 = 4.7 \pm 0.2\%$ which is higher than the value of $2.8 \pm 0.6\%$ reported by Oberli *et al* (1985a, b). Note that our KKR CPA calculations yield values of $\eta(\hat{k})$ which are larger than those obtained by MacDonald's theory. Explanation of this discrepancy is found in the work of Rasolt *et al* (1975) and MacDonald (1980) who have shown that inclusion of non-local mass operators in the theory results in a reduction in the FS distortions for Li by a factor of almost 2; Rasolt *et al* (1975) obtain $\delta = 5.5\%$ for local theory and $\delta = 1.4\%$ for non-local theory, while MacDonald (1980) obtained $\delta = 6.0\%$ for local theory and $\delta = 2.9$ or 3.7%, depending on whether the non-local self-energy correction is used only for the valence part of the self-energy or otherwise. Recalling that our calculations do not include non-local effects, our value of $\delta = 5.6\%$ is in reasonable accord with the local theories of Rasolt *et al* (1975) and MacDonald (1980). The fact that the present 2D ACAR data yield $\delta = 4.7 \pm 0.2\%$ would thus suggest that non-local effects may not be as important for Li as indicated by the earlier work of Oberli *et al* (1985a) which gave $\delta = 2.8 \pm 0.6\%$.

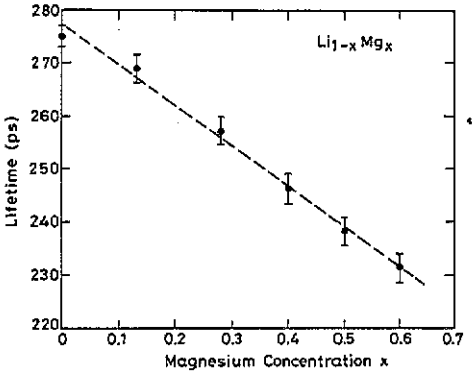

Figure 3. Measured variation in positron lifetimes with x, for the $Li_{1-x}Mg_x$ alloy single crystals used in the experiment.

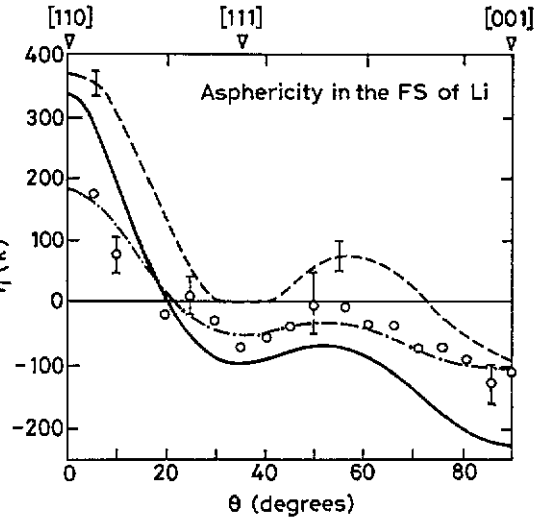

Figure 4. Variation in $\eta(\hat{k})$ (see equation (1)), describing the asphericity in the FS of pure Li, in the $(1\bar{1}0)$ plane. θ denotes the angle between $\hat{k}$ and the [110] direction. The data points are as follows: ——, present KKR CPA theory; – – –, present 2D ACAR experiment; O, 2D ACAR experiment of Oberli *et al* (1985a); — · —, non-local theory of MacDonald (1980).

Figure 5 considers variations in the FS radii of $Li_{1-x}Mg_x$ alloys. Note that no 2D ACAR measurements were made for $x = 0.14$ and 0.22, where theoretical results are nevertheless presented. The experimental and theoretical curves in figure 5 display similar trends,

although the amplitudes of the experimental curves are generally about 2% higher. The discrepancy is, however, somewhat more pronounced for $x = 0.60$ in that the measured points lie above the theoretical values for $0° \leqslant \theta \leqslant 60°$, but below the theoretical values for $60° \leqslant \theta \leqslant 90°$; the origin of this behaviour is unclear.

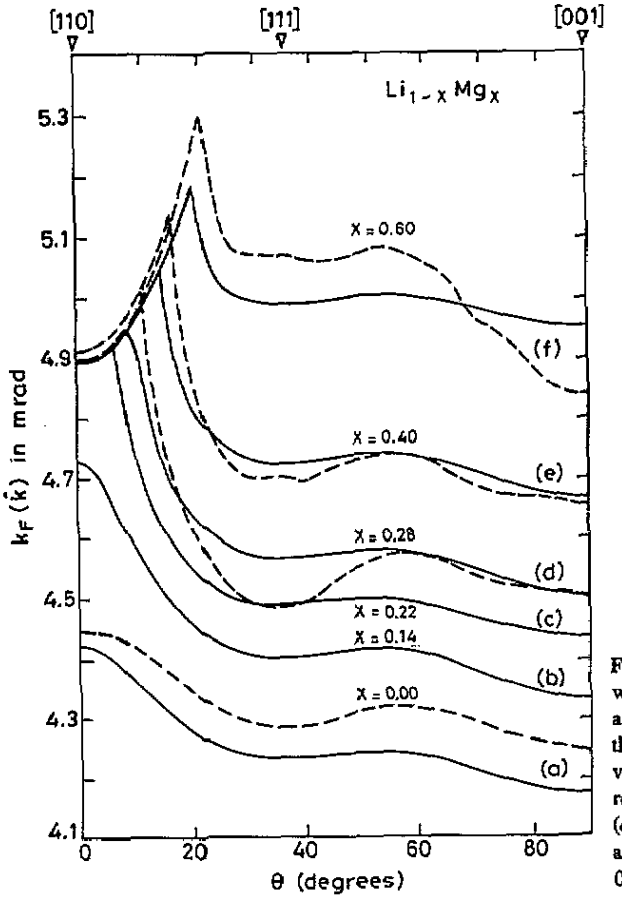

Figure 5. Variation in the FS radius $k_F(\hat{k})$ with θ for $Li_{1-x}Mg_x$ alloys. θ is the same as in figure 4. The full curves (*a*)–(*f*) give the present KKR CPA results for the various x-values indicated. The experimental 2D ACAR results are given by the broken curves (*a*), (*d*), (*e*) and (*f*) for $x = 0.0$, 0.28, 0.40 and 0.60, respectively. Note that 1 mrad = 0.137 au.

Further insight into the FS topology of Li–Mg alloys is provided by figure 6 which shows contour plots of the distribution $\rho^{2\gamma}_{LCW}(k)$ in the $(1\bar{1}0)$ plane, obtained via equation (2) from the measured 2D ACAR data; figure 7 provides a 3D rendition of the FSs. The growth of the FS and the development of the neck (note that because of the periodicity of $\rho^{2\gamma}_{LCW}(k)$ there are four equivalent necks lying at the corners of each part of figure 6), seen clearly in figures 6 and 7, is in good accord with the theoretical results in figure 1.

As mentioned earlier, it is interesting to consider the critical concentration x_c at which the FS first makes contact with the BZ in $Li_{1-x}Mg_x$. In this connection, figure 8 gives a plot of various theoretical and experimental results for the neck radius k_N expressed as the ratio $2k_N/G_{110}$, where G_{110} denotes the distance between the Γ and N points in the BZ. The present KKR CPA results and those of Bruno *et al* (1987) indicate similar trends and both theories predict a neck size smaller than the 2D ACAR measurements. On the other hand the k_N-values deduced by Mathewson and Myers (1973) are substantially smaller than theory, probably because of the inaccuracy of the approximations invoked by these workers

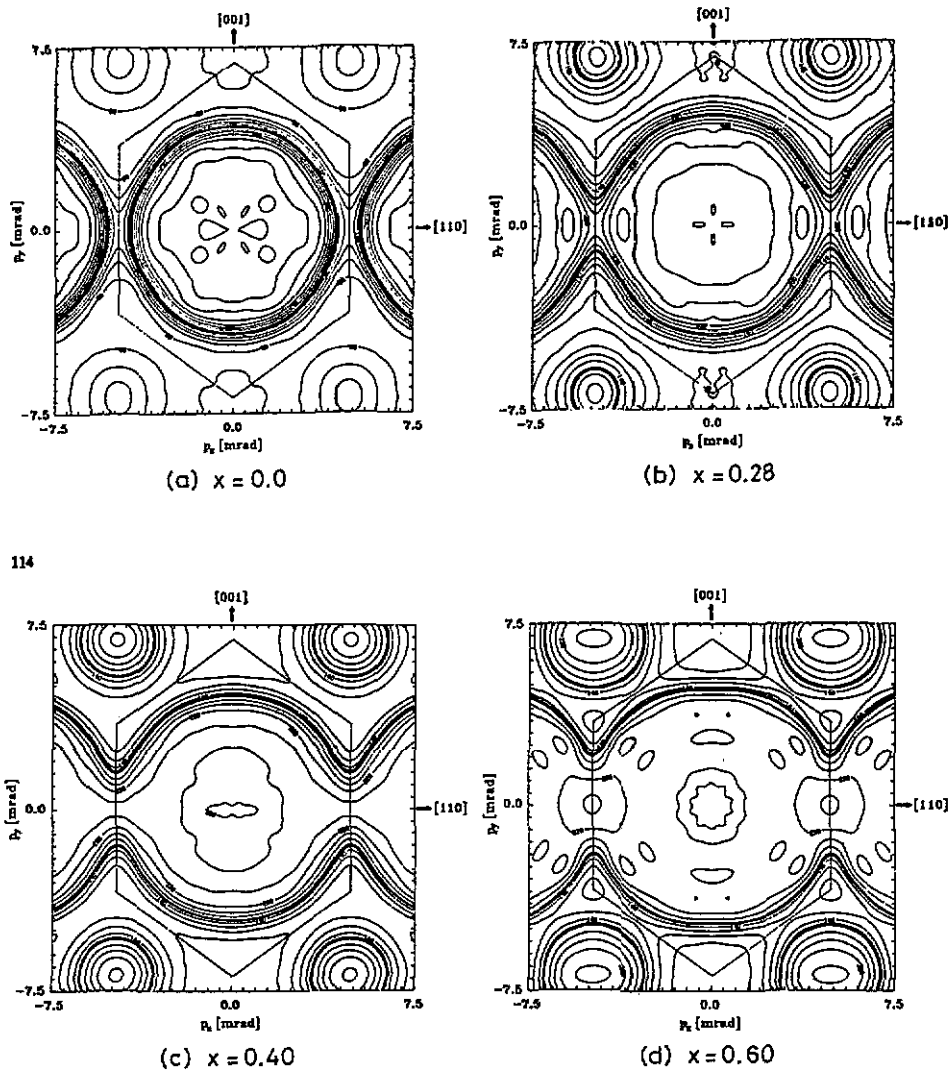

Figure 6. Contour plots of the experimental LCW-folded k-space distribution $\rho^{2\gamma}_{LCW}(k)$ in the $[1\bar{1}0]$ plane for $Li_{1-x}Mg_x$ for various x-values.

in analysing their optical absorption spectra. An extrapolation of our KKR CPA points in figure 8 yields an estimate of $x_c = 0.17 \pm 0.04$ for the critical Mg concentration where the necks first appear for Li–Mg alloys. This theoretical value is in good agreement with the results of thermopower, resistivity and magnetic susceptibility measurements, quoted earlier in this section. A similar extrapolation of the 2D ACAR data points in figure 8 is difficult; further 2D ACAR measurements to determine x_c in the Mg concentration range $x = 0.10$–0.28 would be required. While we plan such experiments with our 2D ACAR machine, we note that the preparation of $Li_{1-x}Mg_x$ single crystals with $x \leqslant 0.28$ poses formidable metallurgical problems.

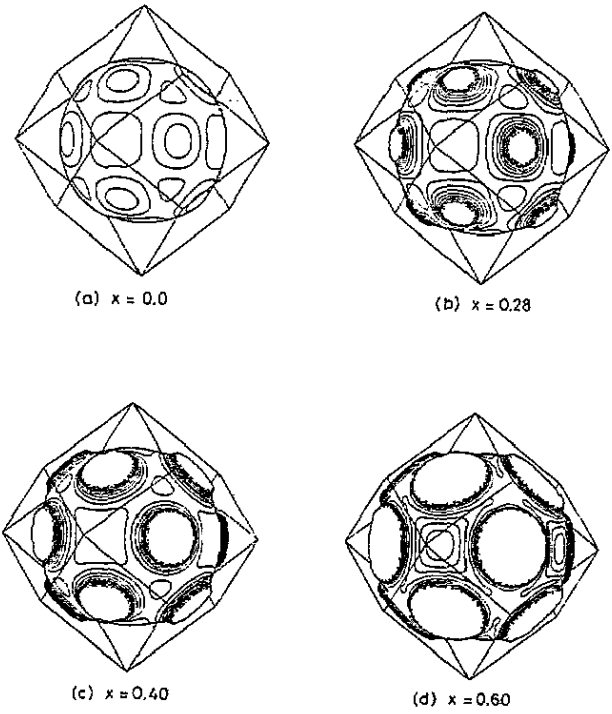

Figure 7. A three-dimensional rendition of the FS of the $Li_{1-x}Mg_x$ alloys for various x-values. The first BZ is indicated. The FS is in contact with the BZ for the cases (*b*), (*c*) and (*d*).

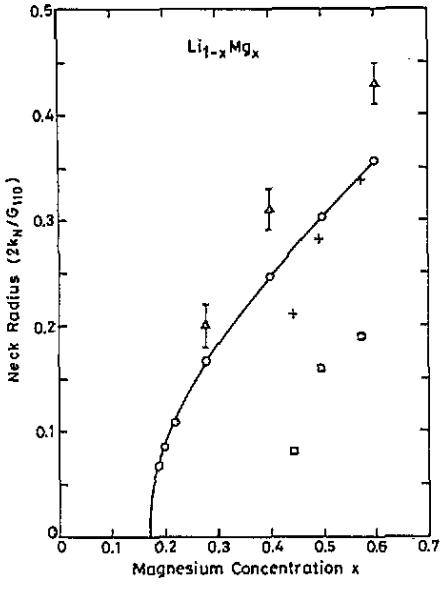

Figure 8. Variation in the neck radius k_N for the FS of $Li_{1-x}Mg_x$ alloys with x expressed as the ratio $2k_N/G_{110}$, where G_{110} is the length of the (110) reciprocal vector. Various data points are as follows: ○, present KKR CPA theory; △, 2D ACAR experiment; +, KKR CPA theory results obtained by Bruno *et al* (1987); □, optical absorption experiment by Mathewson and Myers (1973).

4. Conclusions

A systematic theoretical (KKR CPA) and experimental (2D ACAR) study of the FSs of Li and $Li_{1-x}Mg_x$ ($0.0 < x \leqslant 0.6$) disordered alloys has been carried out. The FS of Li is a

distorted sphere with a bulge along the [110] direction; the FS expands with increasing Mg concentration. On a quantitative level, the overall agreement between our local-density-approximation-based theory and the 2D ACAR experiments with regard to the detailed sizes, shapes and anisotropies of the FSs of $Li_{1-x}Mg_x$ alloys is reasonable, although some discrepancies are observed. The KKR CPA theory predicts that the FS touches the BZ boundary for $0.14 < x < 0.22$, the finite range arising from the disorder-induced smearing of the FS. The present theoretical and experimental results both support the conclusion that a neck in the FS is definitely formed for $x \geqslant 0.28$.

Acknowledgments

We wish to acknowledge valuable discussions with Professor A T Stewart and Dr A A Manuel. One of us (RMS) would like to thank the Alexander von Humboldt Foundation for a fellowship and the Universität der Bundeswehr München for kind hospitality. This work was supported by the Department of Science and Technology, Government of India (grant SP/S2/M-39/87) the US Department of Energy (contract W-31-109-ENG-38, including a subcontract to Northeastern University) and a travel grant from NATO. The computations described here have also benefitted from the allocation of supercomputer time on the ER Cray at NERSC and the Pittsburgh supercomputer centres.

References

Bansil A 1982 *Positron Annihilation* ed P G Coleman, S C Sharma and L M Diana (Amsterdam: North-Holland) p 291
—— 1987 *Electronic Band Structure and its Applications* ed M Yussouff (Berlin: Springer) p 271
—— 1993 *Z. Naturf.* a **48** at press
Bansil A and Kaprzyk S 1991 *Phys. Rev.* B **43** 10335
Bansil A, Kaprzyk S and Tobola J 1992 *Mater. Res. Soc. Symp. Proc.* **253** 505
Basinski S L, Douglas R J and Stewart A T 1979 *Positron Annihilation* ed R R Hasiguti and K Fujiwara (Sendai: Japan Institute of Metals) p 665
Berko S 1983 *Positron Solid State Physics* ed W Brandt and A Dupasquier (Amsterdam: North-Holland) p 64
Berko S, Haghgooie M and Mader J J 1977 *Phys. Lett.* **63A** 335
Berndt K and Brümmer O 1976 *Phys. Status Solidi* b **78** 659
Bross H and Bohn G 1975 *Z. Phys.* B **20** 261
Bruno G, Ginatempo B, Giuliano E S and Stancanelli A 1987 *Nuovo Cimento* D **9** 1495
Callcott T A, Tagle J A, Arakawa E T and Stocks G M 1980 *Appl. Opt.* **19** 4035
Ching W Y and Callaway J 1974 *Phys. Rev.* B **9** 5115
Cooper M, Leake J A and Weiss R J 1965 *Phil. Mag.* **12** 797
Cooper M, Williams B G, Borland R E and Cooper J R A 1970 *Phil. Mag.* **22** 441
Cooper M J 1985 *Rep. Prog. Phys.* **48** 415
Dagens L and Perrot F 1973 *Phys. Rev.* B **8** 1281
Donaghy J and Stewart A T 1967 *Phys. Rev.* **164** 391
Eckert A 1989 *PhD Thesis* Universität der Bundeswehr München, Neubiberg
Egorov V S and Fedorov A N 1983 *Sov. Phys.–JETP* **58** 959
Eisenberger P, Lam J, Platzmann P M and Schmidt P 1972 *Phys. Rev.* B **6** 3671
Herbstein F H and Averbach B L 1956 *Acta Metall.* **4** 407
Ide M 1971 *J. Phys. Soc. Japan* **30** 1352
Kaprzyk S and Bansil A 1990 *Phys. Rev.* B **42** 7358
Kontrym-Sznajd G 1992 *Mater. Sci. Forum* **105–110** 325
Kubica P, McKee B T A, Stewart A T and Stott M J 1975 *Phys. Rev.* B **11** 11
Levinson D W 1958 *A Handbook of Lattice Spacing and Structures of Metals and Alloys* ed W B Pearson (New York: Pergamon) p 715

Lock D G, Crisp V H C and West R N 1973 *J. Phys. F: Met. Phys.* **3** 1675
Lynch G F, Stott M J and Williams A R 1973 *Solid State Commun.* **13** 1675
MacDonald A H 1980 *J. Phys. F: Met. Phys.* **10** 1737
Manuel A A, Oberli L, Jarlborg T, Sachot R, Descouts P and Peter M 1982 *Positron Annihilation* ed P G Coleman, S C Sharma and L M Diana (Amsterdam: North-Holland) p 281
Mathewson A G and Myers H P 1973 *J. Phys. F: Met. Phys.* **3** 623
Mijnarends P E 1969 *Phys. Rev.* **178** 622
—— 1977 *Compton Scattering* ed B Williams (New York: McGraw-Hill) p 323
—— 1987 *Phys. Status Solidi* a **102** 31
Moruzzi V L, Janak J F and Williams A R 1978 *Calculated Electronic Properties of Metals* (Oxford: Pergamon)
Oberli L, Manuel A A, Sachot R, Descouts P and Peter M 1985a *Phys. Rev.* B **31** 6104
Oberli L, Manuel A A, Sachot R, Descouts P, Peter M, Rabou L P L M, Mijnarends P E, Hyodo T and Stewart A T 1985b *Phys. Rev.* B **31** 1147
Oomi G and Woods S B 1985 *Solid State Commun.* **53** 223
Paciga J and Llewelyn Williams D 1971 *Can. J. Phys.* **49** 3227
Pecora L M 1989 *J. Phys.: Condens. Matter* **1** SA 1
Pecora L M, Ehrlich A C, Manuel A A, Singh A K, Peter M and Singru R M 1988 *Phys. Rev.* B **37** 6772
Phillips W C and Weiss R J 1968 *Phys. Rev.* **171** 790
—— 1972 *Phys. Rev.* B **5** 1755
Polmear I J 1981 *Light Alloys* (London: Edwin Arnold)
Prasad R 1991 *Indian J. Pure Appl. Phys.* **29** 255
Prasad R, Papadopoulos S C and Bansil A 1981 *Phys. Rev.* B **23** 2607
Randles D L and Springford M 1976 *J. Phys. F: Met. Phys.* **6** 1827
Rasolt M, Nickerson S B and Vosko S H 1975 *Solid State Commun.* **16** 827
Raynor G V 1959 *The Physical Metallurgy of Magnesium and its Alloys* (London: Pergamon)
Roberts C S 1960 *Magnesium and its Alloys* (New York: Wiley) p 56
Sakurai Y, Nanao S, Nagashima Y, Hyodo T, Iwazumi T, Kawata H, Shiotani N and Stewart A T 1992 *Mater. Sci. Forum* **105–110** 803
Schülke W, Langer T and Lanzki P 1984 *Acta Crystallogr.* A **40** C171
Stewart A 1986 *Positron Studies of Solids, Surfaces and Atoms* ed A Mills Jr, W S Krane and K F Canter (Singapore: World Scientific) p 28
Stewart A T 1964 *Phys. Rev.* **133** 1651
Stocks G M and Winter H 1984 *The Electronic Structure of Complex Systems* ed P Phariseau and W M Temmerman (New York: Plenum) p 463
Svechkarev I V, Sokol O N and Kuz'micheva L B 1977 *Sov. J. Low Temp. Phys.* **3** 77
Triftshäuser W, Eckert A, Kögel G and Sperr P 1992 *Mater. Sci. Forum* **105–110** 501
Vaks V G, Trefilov A V and Fomichev S V 1981 *Sov. Phys.–JETP* **53** 830
Varlamov A A, Egorov V S and Pantsulaya A V 1989 *Adv. Phys.* **38** 469
von Barth U and Hedin L 1972 *J. Phys. C: Solid State Phys.* **5** 1629
Wachtel S, Felsteiner J, Kahane S and Opher R 1975 *Phys. Rev.* B **12** 1285
Young D A and Ross M 1984 *Phys. Rev.* B **29** 682